Structure Parameter Estimation of Smooth-Surfaced Cone-Shaped Precession Target Based on Multi-Station Narrowband Radars

Dan Xu
Academy of Advanced Interdisciplinary Research
Xidian University
Xian, China
danxu@xidian.edu.cn

Ziyi Cao
School of Electronic Engineering
Xidian University
Xian, China
22009100308@stu.xidian.edu.cn

Mengdao Xing
Academy of Advanced Interdisciplinary Research
Xidian University
Xian, China
mdx@xidian.edu.cn

Jiang Qian
School of Resources and Environment
University of Electronic Science and Technology of China
Chengdu, China
jqian@uestc.edu.cn

Fulvio Gini
Department of Information Engineering
University of Pisa
Pisa, Italy
fulvio.gini@unipi.it

Maria Sabrina Greco
Department of Information Engineering
University of Pisa
Pisa, Italy
maria.greco@unipi.it

***Abstract*—This paper presents a novel structural parameter estimation algorithm for smooth-surfaced cone-shaped precession (SSCP) targets based on multi-station narrowband radars. The proposed algorithm leverages Synchro Squeezing Transform (SST) to achieve high-precision micro-motion diagram. The initial phase of the micro-Doppler (MD) frequency and the MD curves are obtained through Inverse Radon and Radon transforms. Subsequently, the algorithm combines any two radars within the network and constructs a compensation function based on the estimated initial phase and the proportional relationship of the target centroid position to compensation the MD signals. An iterative optimization process is employed to estimate the target precession angle and all the radar incident angles. The iteration proceeds until the MD loss function is minimized and the variance of incident angle estimates from multiple radars reaches its lowest value. The algorithm then outputs the target structure parameters along with the incident angle information from each radar. Experimental results validate the reliability and effectiveness of the proposed method, demonstrating that estimation accuracy improves with increasing signal-to-noise ratio (SNR) and the number of radar views.**

Keywords—Structural parameter estimation, smooth-surfaced cone-shaped precession targets, Synchro Squeezing Transform, Radon transform, micro-Doppler frequency.

I. INTRODUCTION

Accurate identification of real and decoy warheads is crucial for missile defense systems. With advancements in target recognition technology, extracting and integrating multidimensional features has become a research focus. When a warhead undergoes precession after release to maintain stability, its radar echoes produce micro-Doppler (MD) modulation, revealing key physical characteristics such as size, mass distribution, and orientation. This modulation is vital for cone-shaped target classification and identification [1], [2]. Additionally, MD effects provide essential information for estimating target structure parameters, but traditional single-station radars are limited by observation angles, making it difficult to fully capture micromotion features [3].

Multi-station radar networks, by integrating MD information from multiple viewing angles, significantly improve target reconstruction accuracy [4], [5]. Although narrowband radars have low range resolution due to bandwidth limitations, they excel at extracting micro-Doppler features [6]. A key challenge in multi-station radar networks is effectively combining echoes from different radars to estimate target structure parameters [7], [8]. Radon transform (RT) based micromotion analysis methods have been proposed to estimate target pose and structure from micro-Doppler features [9]. For example, previous research reconstructed the spatial distribution of scatterers on a cone-shaped warhead using three single-dimensional range profiles, demonstrating the effectiveness of multi-station networks for feature extraction [10] -[12]. However, most existing studies focus on range profile analysis from high-resolution radars, with limited research on MD spectral features from narrowband radar echoes [13], [14]. For smooth-surfaced cone-shaped precession (SSCP) targets, current algorithms struggle to handle their unique micromotion patterns and scatterer characteristics. Hence, there is the need for novel algorithms to leverage multi-station narrowband radar for high-precision structural parameter estimation [15]-[17].

This study proposes a structural parameter estimation algorithm for SSCP targets based on multi-station narrowband radar networks. The algorithm enhances micromotion feature extraction using Synchro Squeezing Transform (SST), Inverse Radon transform (IRT) and applies Radon transform (RT) to obtain multi-angle MD features. By integrating multi-station radar echoes and employing iterative optimization, the algorithm achieves accurate structural parameter estimation. Experimental results demonstrate that the proposed algorithm maintains high accuracy even under low signal-to-noise ratio (SNR) and limited observation angles. This research advances narrowband radar MD feature extraction theory, and provides new insights for target recognition and classification in complex environments.

The novel contributions of this paper are as follows:

(1) Application of SST: compared to Short-Time Fourier Transform (STFT), SST offers higher time-frequency resolution and better energy concentration. STFT suffers from blurring due to its fixed window, while SST improves resolution by estimating instantaneous frequency and redistributing energy. Despite higher computational complexity, SST excels in analyzing non-stationary signals.

(2) Integration of IRT and RT: the integration of IRT and RT effectively separates the intertwined MD frequencies. This is particularly advantageous for resolving the sinusoidal MD variations from the cone vertex scatterer, enabling direct reconstruction of its MD frequency. By efficiently extracting complex multi-frequency components, this approach expands the applicability of the proposed method to scenarios with intricate signal compositions.

(3) The application of multi-station narrowband radar: compared to traditional single-station wideband radar, the use of multi-station narrowband radar provides higher estimation accuracy by utilizing MD, while also reducing the requirements for radar bandwidth.

II. System Model

The geometry of a SSCP target and target coordinate system are illustrated in Fig. 1. Assume that the target precession axis is chosen as the Y-axis. A Cartesian coordinate system is established, with the XOY plane defined by the radar line of sight (LOS) and the precession axis, while the Z-axis is determined using the right-hand rule. The SSCP target height and base radius are *H*, *r*, respectively. The target center of mass is located at *O*. The length between the centroid of cone base and the point *O* is *h*. The incidence angle between the radar LOS and the precession axis is γ .

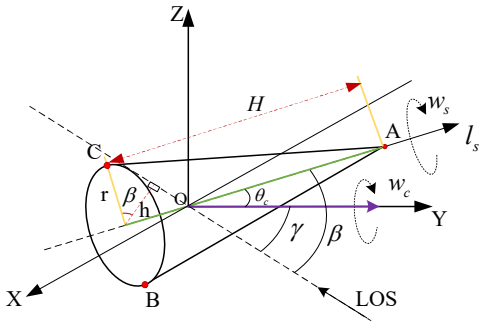

Fig. 1 The motion model of SSCP.

In target coordinate system, the radar LOS can be expressed as

$$\mathrm{L}_{os} = [\sin\gamma, \cos\gamma, 0]. \tag{1}$$

The precession angle refers to the angle between the target precession axis and its axis of symmetry. The precession angle and velocity are denoted by θ_c and w_c, respectively. Then, the initial angle of the target symmetry axis is φ_0, and the target symmetry axis can be represented as

$$ls = [\sin\theta_c \cos(w_c t_m + \varphi_0), \cos\theta_c, \sin\theta_c \sin(w_c t_m + \varphi_0)]. \tag{2}$$

The attitude angle refers to the angle between the radar LOS and the cone axis of symmetry. Due to precession, the attitude angle changes over time:

$$\beta(t_m) = \mathrm{acos}(\sin\gamma \sin\theta_c \cos(w_c t_m + \varphi_0) + \cos\gamma \cos\theta_c). \tag{3}$$

Let $a = \cos\gamma\cos\theta_c$, $b = \sin\gamma\sin\theta_c$, then

$$\cos\beta(t_m) = a + b\cos(w_c t_m + \varphi_0). \tag{4}$$

Then, the radial distance between the radar and the scatterers of the SSCP target can be expressed as

$$r_A(t_m) = R_T(t_m) - H\cos\beta(t_m) + h\cos\beta(t_m), \tag{5}$$

$$r_B(t_m) = R_T(t_m) - r\sin\beta(t_m) + h\cos\beta(t_m), \tag{6}$$

where $R_T(t_m)$ denotes target translation. Assuming that the radar transmits a linear frequency modulation (LFM) signal, after translational compensation and envelope alignment, the signal can be expressed as

$$s(f, t_m) = \sum_{p=A,B} A_p \exp\left(-j\frac{4\pi}{c}(f_c + f)(r_p(t_m) - R_T(t_m))\right), \tag{7}$$

where A_p denotes the amplitude, f_c is the carrier frequency, $f \in [-B_W/2, B_W/2]$, B_W is the bandwidth. Based on (7), the MD of A, B can be calculated as

$$f_{mA}(t_m) = \frac{2w_c}{\lambda}(H - h)b\sin(w_c t_m + \varphi_0), \tag{8}$$

$$f_{mB}(t_m) = -\frac{2}{\lambda}\frac{rbw_c(a + b\cos(w_c t_m + \varphi_0))\sin(w_c t_m + \varphi_0)}{\sqrt{1 - (a + b\cos(w_c t_m + \varphi_0))^2}} - \frac{2}{\lambda}hbw_c\sin(w_c t_m + \varphi_0). \tag{9}$$

III. Structure Parameter Estimation of SSCP Target

A. Scatterers MD Extraction based on SST and IRT

Compared with the traditional STFT method, the SST demonstrates significant advantages in analyzing the MD characteristics of SSCP targets. These advantages include high time-frequency resolution, shift-invariance, strong capability for multi-component signal separation, high energy concentration, and enhanced robustness. By utilizing SST, clearer and more physically meaningful MD signatures can be extracted, even in complex backgrounds with multi-modal interference. Therefore, SST provides strong support for spinning target identification and parameter inversion.

According to (8) and (9), the SSCP target exhibits two MD components: scatterer A presents a sinusoidal MD pattern, while scatterer B shows a quasi-sinusoidal pattern. By applying the IRT transform, these two MD curves can be effectively separated. After the transformation, the well-focused region corresponds to the MD curve of scatterer A, whereas the defocused region corresponds to the MD curve of scatterer B. The mapping relationship is illustrated in Fig. 2. By extracting the positions of the focused peaks and performing the RT transform, the trend curves of the MD signatures for each scatterer can be obtained. Using these trend curves, the individual MD signatures of each scatterer can be reconstructed, enabling accurate MD feature extraction.

In addition, according to the peaks in the IRT, the initial phase of scatterer A and B can be obtained. If the focus position of scatterer A is represented as $(\Delta x_A, \Delta y_A)$, then the initial phase of the MD for scatterer A is expressed as

$$\varphi_A = \begin{cases} \text{atan}\left(\dfrac{\Delta y_A}{\Delta x_A}\right)+\pi, & \begin{matrix}(\Delta y_A>0,\Delta x_A<0)\,or\\ (\Delta y_A<0,\Delta x_A<0)\end{matrix} \\ \text{atan}\left(\dfrac{\Delta y_A}{\Delta x_A}\right), & \text{other wise.} \end{cases} \tag{10}$$

For scatterer B, the initial phase is

$$\varphi_B = \frac{\pi}{2}+\varphi_A \tag{11}$$

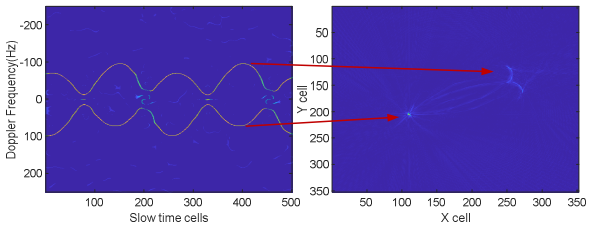

Fig. 2 The Mapping from the SST diagraph of the of SSCP target to the IRT.

B. Structure Parameters estimation

From (8) and (9), it can be seen that due to the influence of the center of mass $R_x = h/(H-h)$, scatterers A and B have a common term $-2hbw_c\sin(w_c t_m+\varphi_0)/\lambda$ in their MD frequencies. Therefore, R_x is the key parameter to be estimated. We can estimate the target parameters by iterating over R_x using the following method. Only when R_x matches the true value will the parameters estimated by the multi-station radar be consistent across all stations. Otherwise, each radar will yield different parameter estimates. Based on the above analysis, the steps of the proposed method can be described as in Fig. 3.

When R_x is set to its true value, the common term is fully removed, we have

$$f_A(t_m) = H\frac{2w_c}{\lambda}b\sin(w_c t_m+\varphi_0), \tag{12}$$

$$f_B(t_m) = -\frac{2}{\lambda}\frac{rbw_c(a+b\cos(w_c t_m+\varphi_0))\sin(w_c t_m+\varphi_0)}{\sqrt{1-(a+b\cos(w_c t_m+\varphi_0))^2}}. \tag{13}$$

Assuming that the network is composed by N radars, we have

$$A_i = \frac{f_{A\_i}(t_m)\big|_{\sin(w_c t_m+\varphi_0)=1}}{f_{A\_1}(t_m)\big|_{\sin(w_c t_m+\varphi_0)=1}} = \frac{\sin\gamma_i}{\sin\gamma_1}, \tag{14}$$

$$B_i = \frac{f_{B\_i}(t_m)\big|_{\sin(w_c t_m+\varphi_0)=1}}{f_{B\_1}(t_m)\big|_{\sin(w_c t_m+\varphi_0)=1}} = \frac{a_i b_i\sqrt{1-a_1^2}}{a_1 b_1\sqrt{1-a_i^2}}, \tag{15}$$

where $f_{A\_i}(t_m)$ and $f_{B\_i}(t_m)$ denotes the MD frequency obtained by the i-th radar after compensation of the common term for the scatterer A and B, respectively.

$f_{A\_i}(t_m)\big|_{\sin(w_c t_m+\varphi_0)=1}$ and $f_{B\_i}(t_m)\big|_{\sin(w_c t_m+\varphi_0)=1}$ represent the values when $\sin(w_c t_m+\varphi_0)=1$. The relationship between their incidence angles is

$$\sin\gamma_i = A_i\sin\gamma_1. \tag{16}$$

The precession angle can be expressed as:

$$\cos\theta_c = \frac{1}{N-1}\sum_{i=2}^{N}\sqrt{\frac{B_i^2}{B_i^2-A_i^2}\left(\frac{1}{1-(A_i\sin\gamma_1)^2}-\frac{1}{\cos\gamma_1^2}\right)}. \tag{17}$$

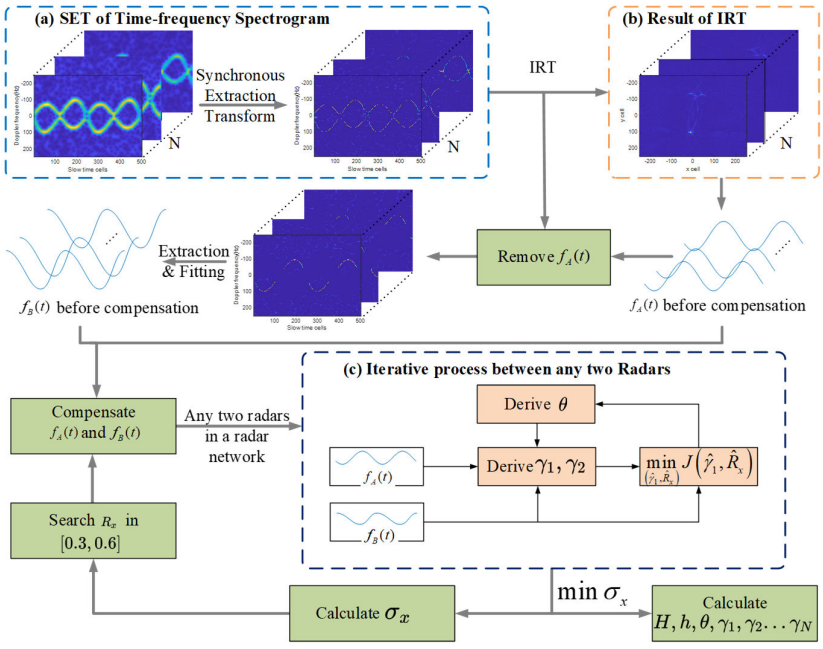

Fig. 3 The flowchart of the proposed algorithm.

Based on the above analysis, the bottom radius r of the target and the distance h from the center of mass to the bottom can be expressed as:

$$r=\frac{1}{N}\sum_{i=1}^{N}\frac{\lambda}{2}\frac{\sqrt{1-a_i^2}}{a_i b_i w_c}f_{B\_i}(t_m)\Big|_{\sin(w_c t_m+\varphi_0)=1}, \quad (18)$$

$$h=\frac{1}{N}\sum_{i=1}^{N}\frac{\lambda}{2b_i w_c}R_x f_{mA\_i}(t_m)\Big|_{\sin(w_c t_m+\varphi_0)=1}. \quad (19)$$

Given r and h, $f_{B\_i}(t_m)$ can be reconstructed. Then, γ_1 and R_x are estimated as follows:

$$J(\hat{\gamma}_1,\hat{R}_x)=\sqrt{\frac{1}{N-1}\sum_{i=2}^{N}w_i\sum_{t_m=-T/2}^{T/2}\left(f_{B\_i}(t_m)-\hat{f}_{B\_i}(t_m)\right)^2}+\lambda\cdot\mathrm{Var}(\hat{\boldsymbol{\gamma}}), \quad (20)$$

where $\hat{f}_{B\_i}(t_m)$ denotes the compensated MD frequency of scatterer B obtained from measurements, $\hat{\boldsymbol{\gamma}}=[\gamma_1,.....,\gamma_N]$, w_i is the weights, λ is the regularization parameter, $\mathrm{Var}(\cdot)$ represents the variance of the parameter estimation. By minimizing (20), the precession angle, centroid position, and the incidence angle of Radar 1 can be estimated. By substituting the estimated results $(\hat{\gamma}_1,\hat{R}_x)$ into (12)-(19), the target structure parameters and the incidence angles of all radars can be obtained.

IV. Experimental Analysis

The goal of the proposed method is to estimate the SSCP target parameters and its attitude in radar coordinates. To quantitatively evaluate the accuracy of the algorithm, we calculate the root mean square error (RMSE):

$$RMSE=\sqrt{\frac{1}{N}\sum_{n=1}^{N}\left(f_e(n)-f_o(n)\right)^2}. \quad (21)$$

The mean relative error (MRE) can be expressed as

$$MRE=\frac{1}{N}\sum_{n=1}^{N}\left|f_e(n)-f_o(n)\right|, \quad (22)$$

where $f_e(n)$ denotes the estimated value, $f_o(n)$ denotes the theoretical value, N denotes the number of experiments.

The SSCP target parameters are set as follows. The distance from the cone vertex to the cone base is $H=1.5m$, the distance from the center to the cone base center is $h=0.5m$, the base radius is $r=0.5m$, and the precession frequency is $f_c=2\mathrm{Hz}$. The radar network parameters are set as in Table I.

TABLE I. Radar Network Parameters

Parameters	Values
Carrier frequency	10GHz
Bandwidth	0.1GHz
Pulse repetition period	500Hz
Observation time	1s
Distance between the radar and target	500Km
Position of radar 1	(0,0,0) Km
Position of radar 2	(-8.763, 41.913, -34.546) Km
Position of radar 3	(73.54, -102.02, 78.99) Km
Position of radar 4	(12.29,82.99, 64.25) Km
Position of radar 5	(44.75, 67.62, 103.18) Km
The angle between the SSCP target precession axis and radar nth LOS	1th γ_1 30°
	2th γ_2 35°
	3th γ_3 25°
	4th γ_4 40°
	5th γ_5 45°

The SNR has a significant impact on MD curve extraction and target parameter estimation. Fig. 4 illustrates four representative time-frequency diagrams for different SNR conditions.

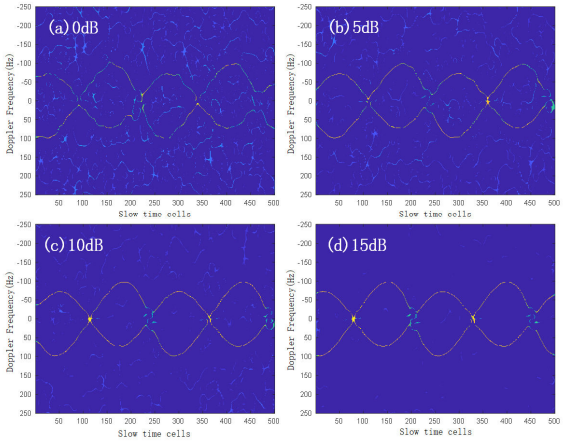

Fig. 4 SST results at different SNRs: (a) 0 dB, (b) 5 dB, (c) 10 dB, (d) 15 dB.

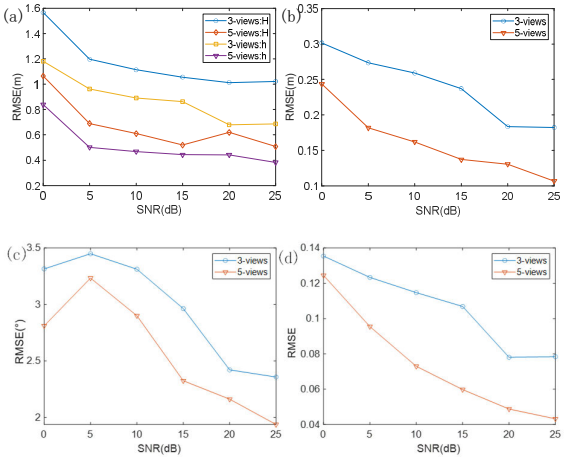

Fig. 5 Target parameter estimation results with 3-view and 5-view under different SNRs: (a) H, h, (b) r, (c) θ, (d) Rx.

Fig. 5 depicts the RMSE of target parameter predictions for six distinct SNR, for both 3-view and 5-view configurations. As shown in Fig. 5, except for the 0 dB SNR case in Fig. 5 (c), the RMSE for both configurations steadily decrease as the SNR increases. In Fig. 5 (c), when the SNR is 0 dB, complex solutions appear in the prediction results of the cone parameters. These complex solutions are automatically eliminated by the program, with an

elimination probability reaching 8%. Consequently, the RMSE of the remaining valid solutions decreases compared to when the SNR is 5 dB. As shown in Fig. 5 (a)–(f), under all given SNR conditions, the RMSE of the cone parameter predictions obtained using 5-view configuration is significantly lower than that obtained using 3-view configuration. These results indicate that increasing the number of views can effectively improve the accuracy of cone parameter predictions.

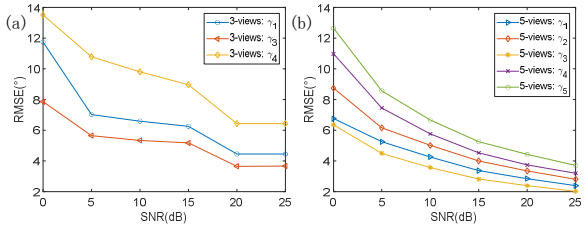

Fig. 6 The estimated RMSE of the angle between the radar LOS and the SSCP target precession axis under different SNRs: (a) 3-view, (b) 5-view.

The estimated RMSE of the angles γ_1 to γ_5 is presented in Fig. 6. The figure also shows that as the SNR increases, the estimation accuracy of all γ_i improves significantly. By comparing the corresponding parameters in Fig. 6 (a) and (b), we observe that as the number of viewing angles increases, the RMSE of the estimated angles decreases by approximately 2°.

In summary, switching the radar view configuration from 3-view to 5-view notably reduces the RMSE of the cone parameters H, h, and r estimation. This reduction exceeds 15% even at an SNR of 0 dB. For γ_1 to γ_5, this reduction exceeds 20%. These results indicate that increasing the number of views can significantly enhance prediction accuracy, even under low SNR conditions.

V. Conclusion

This paper proposes a joint estimation method based on multi-station narrowband radar to extract the characteristic parameters of a SSCP target. The method first employs SST to achieve high-resolution MD estimation. Then, it utilizes IRT and RT to separate and identify MD signals. A cyclic iterative strategy is applied to estimate the target parameters. The precession angle between the target precession axis and the radar LOS is accurately determined by minimizing the cost function and the variance of angle γ. Analysis shows that the algorithm can operate with at least two radars, but its estimation accuracy is relatively low when only two are used. Since the performance of the algorithm is influenced by the SNR and the number of radars, increasing the number of radar perspectives, or improving the SNR, can effectively enhance estimation accuracy. Therefore, future research will focus on multi-station narrowband radar cooperation to further improve estimation reliability and accuracy.

Acknowledgment

This work is supported in part by National Natural Science Foundation of China under grant 62401430, in part by the Fundamental Research Funds for the Central Universities under Grant ZYTS25156.

The work of F. Gini and M.S. Greco has been partially supported by the Italian Ministry of Education and Research (MUR) in the framework of the FoReLab project (Departments of Excellence).

References

[1] V. C. Chen, "Analysis of radar micro-Doppler with time-frequency transform," Proceedings of the Tenth IEEE Workshop on Statistical Signal and Array Processing (Cat. No.00TH8496), Pocono Manor, PA, USA, 2000, pp. 463-466, 2000.

[2] V. C. Chen, C.-T. Lin and W. P. Pala, "Time-varying Doppler analysis of electromagnetic backscattering from rotating object," *2006 IEEE Conference on Radar*, Verona, NY, USA, pp. 6,2006.

[3] Feng Cun-qian, Li Jing-qing, He Si-san, Zhang Hao. "Micro-Doppler Feature Extraction and Recognition Based on Netted Radar for Ballistic Targets," Journal of Radars, vol.4, no.6, pp. 609-620, 2015.

[4] X. Tian, X. Bai, R. Xue, R. Qin, F. Zhou. "Fusion Recognition of Space Targets with Micro-Motion," in IEEE Transaction on Aerospace and Electronic Systems, vol.58, no.4, pp. 3116-3125, 2022.

[5] Zhao Shuang, Lu Weihong, Feng Cunqian, Wang Yizhe. "Three-Dimensional Precession Feature Extraction of Ballistic Targets Based on Narrowband Radar Network," Journal of Radars, vol.6, no.1, pp. 98-105, 2017.

[6] S. Zhao, J. Niu, X. Li and C. Qiao, "Improved HHT and its application in narrowband radar imaging for precession cone-shaped targets," in *Journal of Systems Engineering and Electronics*, vol. 25, no. 6, pp. 977-986, Dec. 2014

[7] F. Zhou, M. Xing, X. Bai, G. Sun and Z. Bao, "Narrow-Band Interference Suppression for SAR Based on Complex Empirical Mode Decomposition," in *IEEE Geoscience and Remote Sensing Letters*, vol. 6, no. 3, pp. 423-427, July 2009.

[8] K. Li, X. Dai, Y. Luo, et al. "Review of radar micro-motion feature extraction and recognition for ballistic targets". Journal of Air Force Engineering University, vol.24, no.1, pp. 6-17, 25, 2023.

[9] Y. Liu, H. Chen, X. Li, et al. "Radar micro-motion target resolution". 2006 International Conference on Radar. Shanghai, China, pp. 1-4.

[10] Z. Wang, F. Sun, X. Zhao, Y. Luo, H. Yuan and Q. Zhang, "3D Micro-Motion Parameter Extraction of Spinning Targets Based on Rotating Antenna," 2022 IEEE 5th International Conference on Electronic Information and Communication Technology (ICEICT), Hefei, China, 2022, pp. 624-629.

[11] Y. Zhang, Q. Zhang, L. Kang, Y. Luo and L. Zhang, "End-to-End Recognition of Similar Space Cone–Cylinder Targets Based on Complex-Valued Coordinate Attention Networks," in IEEE Transactions on Geoscience and Remote Sensing, vol. 60, pp. 1-14, 2022.

[12] H. Yuan, S. -Y. Zhao, Y. -J. Chen, Y. Luo, Y. -X. Liu and Y. -P. Zhang, "Micromotion Parameters Estimation of Precession Cone Based on Monostatic Radars," in IEEE Transactions on Antennas and Propagation, vol. 72, no. 3, pp. 2811-2824, March 2024.

[13] D. Xu, J. Fu, G-C. Sun, M. Xing, T. Su, "Accurate wide band high velocity motion compensation for ballistic targets", Systems Engineering and Electronics. Vol. 41, no.10, pp. 2205-2213, 2019.

[14] Y. Zhu, W. Zhang, H. Yi, and H. Xu. "Enhanced Root-MUSIC Algorithm Based on Matrix Reconstruction for Frequency Estimation," in Sensors, vol. 23, no. 4, pp. 1829, 2023.

[15] Y. Luo, Y. Chen, Y. Zhu, et al. "Doppler effect and micro-Doppler effect of vortex-electromagnetic-wave-based radar," in IET Radar, Sonar & Navigation, 2020, 14, 2-9.

[16] H. Yuan, S. -Y. Zhao, Y. -J. Chen, Y. Luo, Y. -X. Liu and Y. -P. Zhang, "Micromotion Parameters Estimation of Precession Cone Based on Monostatic Radars," in IEEE Transactions on Antennas and Propagation, vol. 72, no. 3, pp. 2811-2824, March 2024.

[17] X. Bai, F. Zhou, Z. Bao. "High-Resolution Three-Dimensional Imaging of Space Targets in Micromotion," in IEEE Journal of Selected Topics in Applied Earth Observations and Remote Sensing, vol.8, no.7, pp. 1-13, 2017.